J Electr Eng Technol Vol. 8, No. 3: 478-489, 2013
http://dx.doi.org/10.5370/JEET.2013.8.3.478

ISSN(Print) 1975-0102
ISSN(Online) 2093-7423

Designing an Emotional Intelligent Controller for IPFC to Improve the Transient Stability Based on Energy Function

Ehsan jafari†, Ali Marjanian*, Soodabeh Solaymani* and Ghazanfar Shahgholian**

Abstract – The controllability and stability of power systems can be increased by Flexible AC Transmission Devices (FACTs). One of the FACTs devices is Interline Power-Flow Controller (IPFC) by which the voltage stability, dynamic stability and transient stability of power systems can be improved. In the present paper, the convenient operation and control of IPFC for transient stability improvement are considered. Considering that the system's Lyapunov energy function is a relevant tool to study the stability affair. IPFC energy function optimization has been used in order to access the maximum of transient stability margin. In order to control IPFC, a Brain Emotional Learning Based Intelligent Controller (BELBIC) and PI controller have been used. The utilization of the new controller is based on the emotion-processing mechanism in the brain and is essentially an action selection, which is based on sensory inputs and emotional cues. This intelligent control is based on the limbic system of the mammalian brain. Simulation confirms the ability of BELBIC controller compared with conventional PI controller. The designing results have been studied by the simulation of a single-machine system with infinite bus (SMIB) and another standard 9-buses system (Anderson and Fouad, 1977).

Keywords: Emotional learning, Interline Power-Flow Controller(IPFC), Transient stability, Critical Clearing Time (CCT).

1. Introduction

Planning and stabilizing are two important problems for the promotion of power system performance, that increasing the demands, in one hand, and the limitations of the new lines formation, on the other hand, can increase the risk of losing stability after occurring a turbulence.

If the turbulence amplitude be great, the stability will be discussed as transient stability. Critical Clearing Time (CCT) if the disturbance is great, the stability will be discussed as the transient stability.CCT has been used for studying transient stability, which CCT enhancement denotes on transient stability improvement. By development of power electronic, the technology of FACTs devices was originated based on using controllable power electronic devices [1-4]. Furthermore**,** many controllers have been used to control FACTs devices. Among these controllers, those designed for linear model in special work points can be mentioned. The functionality of Lyapunov stability direct method has been studied in 1980s [5-7]. Reference [8] is the basis of many studies accomplished in applying Lyapunov function in the power networks for FACTs devices. In [9], with the aim of accessing to maximum of the transient stability limit, the maximization of the network total potential energy has been considered by defining the critical energy function for UPFC and controlling UPFC adequately.

Also, there are some studies relating to the functionality of the Lyapunov direct method for controlling UPFC with the aim of damping the system oscillations [10]. IPFC was introduced by Gyugyi in 1999 for the first time [11]. [12-13] has compared IPFC with the other FACTs devices, and the rate of its efficacy has been compared with the other multi-convertor devices. In [14-16], the various operations of IPFC are described, and IPFC control structure is described in order to control the power transmission in the steady state. In [17], system energy function with IPFC has been calculated using IPFC injected model and it has used nominal instances of Lyapunov direct method for assessing the transient stability. However, it has not been perorated any special control method for reaching the maximum of IPFC injected energy to network and stability margin. In controlling FACTs devices, intellectual systems are quickly considered. For instance, utilizing UPFC fuzzy control with the aim of improving transient stability can be mentioned**.** In [18], UPFC intellectual control has been studied via designing two fuzzy controllers. One controller was used for calculating essential power for transient stability improvement, and the other for controlling UPFC parameters with the aim of producing the calculated power. In some papers, the application of Neuro networks in controlling FACTs devices, such as UPFC, has been studied [19]. In [20]**,** it is considered controlling UPFC by Nero network based on Lyapunov in order to improve

† Corresponding Author: Dept. of Electrical Engineering, Science and Research Branch, Islamic Azad University, Tehran, Iran. (ehsanjafari32 @yahoo.com).
* Dept. of Electrical Engineering, Science and Research Branch, Islamic Azad University, Tehran, Iran. ({marjanian_powerelectronics, soodabeh_ soleymani}@ yahoo.com).
** Dept. of Electrical Engineering, Najafabad Branch, Islamic Azad University, Isfahan, Iran (shahgholian@iaun.ac.ir)
Received: January 22, 2012; Accepted: January 3, 2013

power system transient stability. In [21], SSSC, STATCOM, and UPFC have been controlled by the radial basis function network (RBFN) controller, and their function has been compared in transient stability improvement.

According to the review in [22], several attempts have been made to model the emotional behavior of the human brain [23, 24]. In [24], the computational models of the amygdala and context processing were introduced, which were named Brain Emotional-Learning (BEL) model, which was not used in any practical area, particularly in engineering applications. Based on the cognitively motivated open-loop model, the BEL-based intelligent controller (BELBIC) was introduced for the first time by Lucas in 2004 [25], and during the past few years, this controller has been used in control devices for several industrial applications such as heating, ventilating, and air conditioning control problems, washing machines, controlling a mobile crane and electrical machine drives [26-32]. The main features of that controller were its enhanced learning capability, provision of a model-free control algorithm, robustness, and ability to respond swiftly.

For the first time, the implementation of the BELBIC method for electrical drive control was presented by Rahman *et al.* [33]. In [34], Markadeh *et al,* used a modified emotional controller for the simultaneous speed and flux control of a laboratory IM drive. This simultaneous speed and flux control is achieved by quick auto learning and adaptively proper tracking of reference speed and is quite independent of system parameters, which results in performance improvement. Moreover, many other advantages of the BELBIC are investigated in other electric drives in [35]. [36], is the only paper which study the application of Belbic on the power system.

In this paper, IPFC energy function optimization is considered in order to reach the maximum amount of transient stability margin. This idea is the basis of adjust Emotional Intelligent and PI controller parameters as IPFC controller; also, transient stability has been studied by calculating CCT parameter.

2. System Model

2.1 Interline Power-Flow Controller(IPFC)

IPFC is one of the FACTs devices, which compensates of two or more transmission lines simultaneously; each line is compensated by inserting a series voltage source by applying a voltage-source convertor (VSC). All converters are connected to a DC link that includes a condenser. In this method, the active power can be exchanged between the compensated lines; it is shown in Fig. 1. It shows the model of an IPFC for n compensated lines. The functionality of IPFC can be described by a single-line diagram which includes one IPFC. Fig. 2(a) shows the base diagram, and Fig. 2(b) shows the phasor diagram of such a line. Reactance X_{TRS} is the sum of the reactance of IPFC's series transformer and the line reactance. The system has been considered to be lossless. It should be noted that the amplitude of the series voltage injected by IPFC (U_T) depends on the amplitude of the bus voltage U_i. Thus, the control parameters of each IPFC's branch are the amplitude and the angle of series voltage injected by VSC (i.e., U_T, φ_T). By changing these two parameters, the other system parameters will be changed. In Fig. 2(a), Q_T is the reactive power provided by a VSC, while P_T is the active power provided by DC circuit from other branches. In the other words, in an IPFC consisting of n branches, 2n-1 parameters can be independently controlled, while one parameter has to provide active power balance of a device. In the phasor diagram, in Fig. 2(b), the inner lines of the circle are the constant active-injected power lines. This means that if U_T is controlled in a way that its end is placed on this line, active power injected by converter will be constant; therefore**,** it proves that this line is parallel with the line which connects two ends of voltages U_i and U_j together. Fig. 2(b) shows that the control filed of IPFC series branch is restricted to the maximum amplitude of voltage U_{TMAX}. The equations for the active and reactive powers as functions of the system and the IPFC's

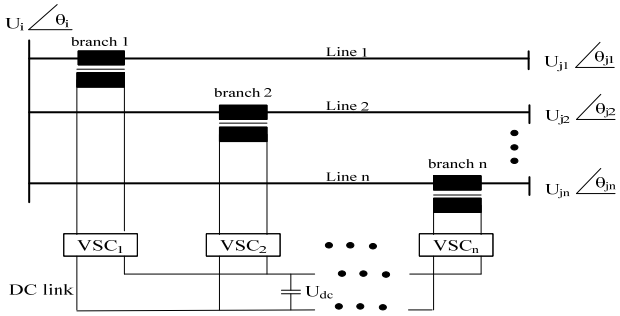

Fig. 1. Model of an IPFC consisting of *n*-series branches

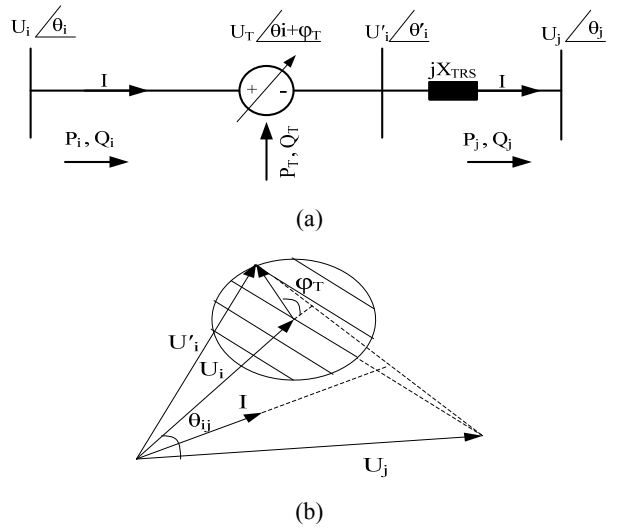

Fig. 2. Single compensated line: (a) functional scheme; (b) phasor diagram.

controllable parameters for a single compensated line according to Fig. 2 can be obtained after some algebraic calculations. They are calculated by Eqs. (1)-(6).

$$P_i=\frac{U_i.U_j.\sin(\theta_{ij})+U_i.U_T.\sin(\varphi_T)}{X_{TRS}} \quad (1)$$

$$Q_i=\frac{U_i^2.U_i.U_j+U_i.U_T\sin\varphi_T}{X_{TRS}} \quad (2)$$

$$P_j=\frac{U_i.U_j.\sin(\theta_{ij})+U_j.U_T.\sin(\theta_{ij}+\varphi_T)}{X_{TRS}} \quad (3)$$

$$Q_i=\frac{-U_j^2.U_i.U_j.\cos(\theta_{ij})+U_j.U_T.\cos(\theta_{ij}+\varphi_T)}{X_{TRS}} \quad (4)$$

$$P_T=-\frac{U_T.(U_i\sin(\varphi_T)-U_j\sin(\theta_{ij}+\varphi_T))}{X_{TRS}} \quad (5)$$

$$Q_T=\frac{U_T.(U_T+U_i.\cos(\varphi_{T1})-U_j.\cos(\theta_{ij}+\varphi_{T)})}{X_{TRS}} \quad (6)$$

The sum of active powers injected into all the series branches must be equal to zero.

$$\sum_{i=1}^{n} P_{Ti}=0 \quad (7)$$

In this paper, for simplicity, IPFC is shown by VSC which compensates two lines. In the next equations, denote 1 is considered for the first branch and 2 for the second branch. Voltages U_{i1} and U_{i2} connect to a shared loop and have equal voltage. But voltages U_{j1} and U_{j2} are different. Access to energy function is needed, so IPFC should be modeled as an injected model. The injected model of each IPFC branch is similar to the injected model shown in [13]. By connecting two branches to a shared DC link, IPFC injected model has been shown in Fig3. Since the IPFC controllable parameters are the amplitude and series injected voltage phase in each branch, so four parameters U_{T1} ,U_{T2} ,φ_{T1} and φ_{T2} are generated, which according to (7), these parameters are not independent of each other. The injected active and reactive powers are calculated in the injected model based on (8)-(15).

$$P_{si1}=\frac{U_iU_{T1}}{X_{TRS1}}\sin(\varphi_{T1}) \quad (8)$$

$$P_{si2}=\frac{U_iU_{T2}}{X_{TRS2}}\sin(\varphi_{T2}) \quad (9)$$

$$P_{sj1}=-\frac{U_{j1}U_{T1}}{X_{TRS1}}\sin(\theta_{ij1}+\varphi_{T1}) \quad (10)$$

$$P_{sj2}=-\frac{U_{j2}U_{T2}}{X_{TRS2}}\sin(\theta_{ij2}+\varphi_{T2}) \quad (11)$$

$$Q_{si1}=\frac{U_iU_{T1}}{X_{TRS1}}\cos\varphi_{T1} \quad (12)$$

$$Q_{si2}=\frac{U_iU_{T2}}{X_{TRS2}}\cos\varphi_{T2} \quad (13)$$

$$Q_{sj1}=-\frac{U_{j1}U_{T1}}{X_{TRS1}}\cos(\theta_{ij1}+\varphi_{T1}) \quad (14)$$

$$Q_{sj2}=-\frac{U_{j2}U_{T2}}{X_{TRS2}}\cos(\theta_{ij2}+\varphi_{T2}) \quad (15)$$

The injected powers of the injected model are very important in obtaining an IPFC energy function.

2.2 Energy function

The energy function for an IPFC contains two series branches extendable to IPFC with n arbitrary series branches. The energy function, on a structure-preserving frame for power system without FACTs devices was developed in 1980. For obtaining the system energy function with an IPFC, the modified oscillation equations should be integrated. As, the energy function can be obtained by the integration of sum of modified equations, which is presented in [14]; therefore, the injected active powers, in (8)-(11), are multiplied with the time derivative of bus voltage angle. Also, the injected reactive powers, in (12)-(15), are divided by the bus voltage magnitude and multiplied with the time derivative of bus voltage magnitude. Since the active power is not injected by IPFC to the network, therefore, for an IPFC with two series branches results as:

$$P_{si1}+P_{si2}=-(P_{sj1}+P_{sj2}) \quad (16)$$

According to (16), the following equations can be obtained:

$$(P_{si1}+P_{si2}).\dot{\theta}_i=$$
$$[\frac{U_{j1}U_{T1}}{X_{TRS1}}\sin(\theta_{ij1}+\varphi_{T1})+\frac{U_{j2}U_{T2}}{X_{TRS2}}\sin(\theta_{ij2}+\varphi_{T2})].\dot{\theta}_i \quad (17)$$

$$P_{sj1}.\dot{\theta}_{j1}=-\frac{U_{j1}U_{T1}}{X_{TRS1}}\sin(\theta_{ij1}+\varphi_{T1}).\dot{\theta}_{j1} \quad (18)$$

$$P_{sj2}\dot{\theta}_{j2}=-\frac{U_{j2}U_{T2}}{X_{TRS2}}\sin(\theta_{ij2}+\varphi_{T2}).\dot{\theta}_{j2} \quad (19)$$

$$\frac{Q_{si1}+Q_{si2}}{U_i}\dot{U}_i=\frac{\dot{U}_iU_{T1}}{X_{TRS1}}\cos(\varphi_{T1})+\frac{\dot{U}_iU_{T2}}{X_{TRS2}}\cos(\varphi_{T2}) \quad (20)$$

$$\frac{Q_{sj1}}{U_{j1}}\dot{U}_{j1}=-\frac{\dot{U}_{j1}U_{T1}}{X_{TRS1}}\cos(\theta_{ij1}+\varphi_{T1}) \quad (21)$$

$$\frac{Q_{sj2}}{U_{j2}}\dot{U}_{j2}=-\frac{\dot{U}_{j2}U_{T2}}{X_{TRS2}}\cos(\theta_{ij2}+\varphi_{T2}) \quad (22)$$

The sum of (17)-(22) can be rewritten as:

$$(P_{si1}+P_{si2}).\dot{\theta}_i+P_{sj1}.\dot{\theta}_{j1}+P_{sj2}\dot{\theta}_{j2}+\frac{Q_{si1}+Q_{si2}}{U_i}\dot{U}_i+$$
$$\frac{Q_{sj1}}{U_{j1}}\dot{U}_{j1}+\frac{Q_{sj2}}{U_{j2}}\dot{U}_{j2}=\frac{U_{j1}.U_{T1}}{X_{TRS1}}\sin(\theta_{ij1}+\varphi_{T1}).\dot{\theta}_{ij1}+$$
$$Uj2.UT2.XTRS2\sin(\theta ij2+\varphi T2)\theta ij2+UiUT1.XTRS1\cos(\varphi T1)+$$
$$\frac{\dot{U}_iU_{T2}}{X_{TRS2}}\cos(\varphi_{T2})-\frac{\dot{U}_{j1}U_{T1}}{X_{TRS1}}\cos(\theta_{ij1}+\varphi_{T1})-$$
$$\frac{\dot{U}_{j2}U_{T2}}{X_{TRS2}}\cos(\theta_{ij2}+\varphi_{T2}) \quad (23)$$

A crucial step in energy function construction is how to obtain an analytical solution of the first integral of (23).

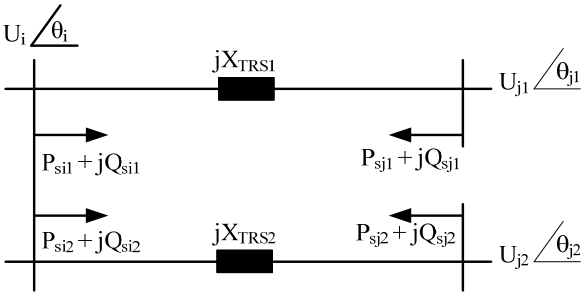

Fig. 3. IPFC injected powers model with two series branches.

However**,** there is no uniform procedure to calculate this integral. For any kind of FACTs devices, there is a procedure to solve which depends on the controllable strategy.

Thus, there is no uniform procedure to obtain a Lyapunov energy function. According to the energy function obtained for the other FACTs devices in [17], it can be found that energy functions for some of the FACTs devices are very closely related to the reactive powers injected into the system. For FACTs devices that operate as controllable current or voltage source, the energy function is equal to the total sum of the reactive-power injected, and the energy function for FACTs devices that operate as controllable reactance, the energy function is equal to half of the sum of the reactive powers injected into the system by these devices. Therefore, the sum of the IPFC's reactive-power injections is equal to:

$$Q_{inj} = Q_{si1} + Q_{si2} + Q_{sj1} + Q_{sj2} \tag{24}$$

The next step is to find the time derivative of the (24), and compare it with (23), it can be seen that all parts of the (23), are included in this derivative. The first integral of (23), which represents the energy function for an IPFC, can now be rewritten as:

$$V_{IPFC} = Q_{inj} - \int [\frac{U_i \dot{U}_{T1}}{X_{TRS1}} \cos\varphi_{T1} - \frac{U_i U_{T1}}{X_{TRS1}} \sin(\varphi_{T1})\dot{\varphi}_{T1} + UiUT2XTRS2\cos(\varphi T2) - UiUT2XTRS2\sin(\varphi T2)\varphi T2 - Uj1UT1XTRS1\cos(\theta ij1+\varphi T1) + \frac{U_{j1}U_{T1}}{X_{TRS1}}\sin(\theta_{ij1}+\varphi_{T1})\dot{\varphi}_{T1} - \frac{U_{j2}\dot{U}_{T2}}{X_{TRS2}}\cos(\theta_{ij2}+\varphi_{T2}) + \frac{U_{j2}U_{T2}}{X_{TRS2}}\sin(\theta_{ij2}+\varphi_{T2})\dot{\varphi}_{T2}]dt \tag{25}$$

So, if U_{T1} and $U_{T2}$are set in their maximum value and φ_{T1} is fixed, and considering that φ_{T2} is dependent to three other parameters, IPFC Lyapunov energy function will be definable for the first oscillation. It is clear that applying IPFC with fixed parameters won't be so important in transient stability improvement. However, [17] has shown that if IPFC's parameters would be controlled as a sectional constant, the energy function definition is correct. Thus, Eq. (25) can be simplified as (26).

$$V_{IPFC} = Q_{inj} + \int [\frac{U_i U_{T2}}{X_{TRS2}} \sin(\varphi_{T2}) - \frac{U_{j2}U_{T2}}{X_{TRS2}} \sin(\theta_{ij2} + \varphi_{T2})]d\varphi_{T2} \tag{26}$$

By replacing (5) in (26), calculated (27).

$$V_{IPFC} = Q_{inj} + \int P_{T2} d_{\varphi T2} \tag{27}$$

3. Control Method

As pointed previously, when the purpose is transient stability improvement, two controllable parameters U_{TI} and U_{T2} must be set in their maximum value proportional to the selective rated values; in the other words, after selecting IPFC rated voltage and power, two parameters from four controllable parameters will be marked. So, it just remains parameters $\varphi_{T1}$and φ_{T2}. On the other hands, the more energy IPFC injects to the network, the more transient stability security margin will be. Thus, IPFC the optimized energy function is used to control IPFC to improve the transient stability. In this way that φ_{T1} is determined so that IPFC energy function will be maximized in (26). As, for obtaining φ_{TI}, by which the energy function is maximized, the derivative of the energy function should be done towards φ_{T1}, considering that φ_{T2} is fixed.

$$\frac{dV_{IPFC}}{d\varphi_{T1}} = 0 \tag{28}$$

$$\frac{U_{T1}.U_i}{X_{TRS1}}\sin(\varphi_{T1}) + \frac{U_{T1}U_{j1}}{X_{TRS2}}\sin(\theta_{ij1} + \varphi_{T1}) = 0 \tag{29}$$

If $X_{TRS2} = X_{TRS1} = 0.1\ P.U,\ U_{J2} = U_{j1} = 1P.U,\ \theta_{ij2} = \theta_{ij1} = \theta_i = \delta$, hence:

$$-U_i \sin(\varphi_{T1}) + \sin(\delta + \varphi_{T1}) = 0 \tag{30}$$

φ_{T1} is calculated by (31).

$$\varphi_{T1} = -\frac{i}{2}\log[\frac{U_i - e^{-\delta i}}{U_i - e^{\delta i}}] \tag{31}$$

And, according to (7) - (11),

$$U_i \sin(\varphi_{T1}) + U_i \sin(\varphi_{T2}) - \sin(\delta + \varphi_{T1}) - \sin(\delta + \varphi T2) = 0 \tag{32}$$

If φ_{T1}, be clear then φ_{T2} can be also calculated.

3.1 Computational model of BELBIC system

Motivated by the success in the functional modeling of emotions in control engineering applications [22-33], the main purpose of this paper is to use a structural model based on the limbic system of the mammalian brain and its learning process for the control of an IPFC. The network connection structure of the mammalian brain developed by Moren and Balkenius [23, 24] is utilized in this paper as a computational model that mimics the amygdala,

orbitofrontal cortex, thalamus, sensory input cortex, and, generally, those parts of the brain thought to be responsible for processing emotions. Fig. 4 shows the pertinent pictures of the human brain [34]. Fig. 5 shows a graphical depiction of the modified sensory signal and learning network connection model inside the brain. The neurobiological aspects of the amygdala, orbitofrontal cortex, thalamus, hippocampus, and associated areas are relevant for the functional and computational perspectives of the emotional responses. The small almond-shaped subcortical area of the amygdala in Fig. 4 is well placed to receive stimuli from all sensory cortices and other sensory areas of the hippocampus in the brain [31]. There are two approaches to intelligent and cognitive control, namely, direct and indirect approaches. In the indirect approach, the intelligent system is utilized for tuning the parameters of the controller. One can adopt the direct approach via using the computational model as a feedback control system for the series branches voltage angle control of an IPFC. The intelligent computational model termed BELBIC is used as the controller block [25]. For the sake of simplicity, the BELBIC is called emotional controller in this paper. The model of the proposed BELBIC input and output structure is shown in Fig. 5. The BELBIC technique is essentially an action-generation mechanism based on sensory inputs and emotional cues. In an IPFC, the choice of the sensory inputs (feedback signals) is selected for control judgment whereas the choice of the emotional cues depends on the performance objectives in IPFC applications. In general, these are vector-valued quantities. For the sake of illustration, one sensory input and one emotional signal (stress) have been considered in this paper. The emotional learning occurs mainly in the amygdala. It has been suggested that the relation between a stimulus and its emotional consequences takes place in the amygdala part of the brain [37]. The amygdala is a part of the brain that must be responsible for processing emotions and must correspond with the orbitofrontal cortex, thalamus, and sensory input cortex in the network model. The amygdala and the orbitofrontal cortex have a network like structure, and within the computational model of each of them, there is one connection in lieu of each sensory input. Also, there is another connection for thalamus input within the amygdala. The value of this input is equal to the maximum value of the sensory inputs. The equivalent network connection in Fig. 5 is described by the control s tructure of human brain in the following Fig. 6. There is one *A* node for every stimulus *S*, including one for the thalamic stimulus.

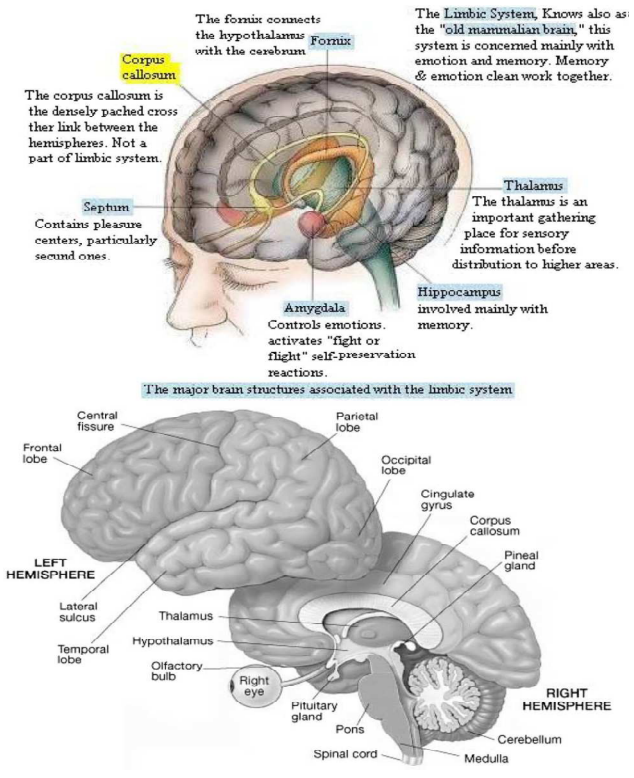

Fig. 4. Sectional view of the human brain for emotion process

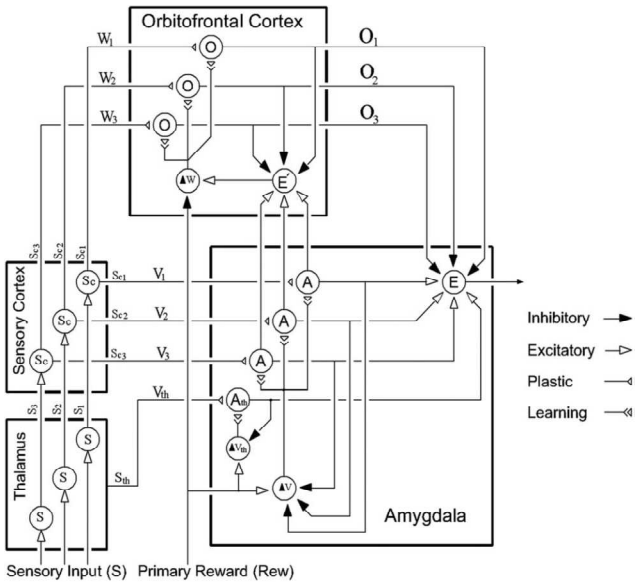

Fig. 5. Graphical depiction of the developed network model of the BEL

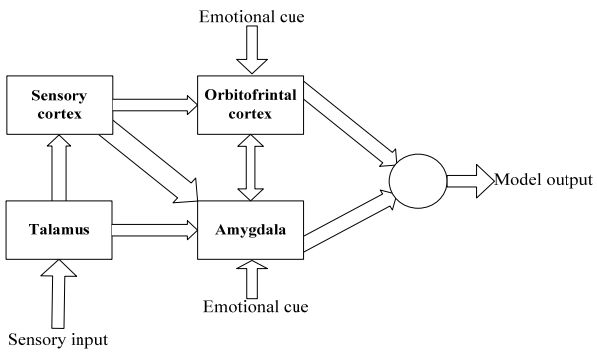

Fig. 6. Structure of the computational model mimicking some parts of the mammalian brain.

There is also one O node for each of the stimuli, except for the thalamic node. There is one output node E that is common for all the outputs of the model.

The E node simply sums the outputs from the A nodes and then subtracts the inhibitory outputs from the O nodes.

The result is the output of the closed-loop model. In other words, the output E of the emotional controller can be obtained from the following:

$$E = \sum_j A_j + A_{th} - \sum_j O_j \tag{33}$$

The internal area outputs are computed pursuant to

$$A_{th} = V_{th}.[\max(S_j) = S_{th}] \tag{34}$$

$$A_j = V_j.S_j \tag{35}$$

$$O_j = W_j.S_j \tag{36}$$

$$Sc_j = S_j \otimes e^{-kt} \tag{37}$$

Where A_j and O_j are the values of amygdala output and the output of the orbitofrontal cortex at each time, V_j is the gain in the amygdala connection, W_j is the gain in the orbitofrontal connection, S_j and S_{cj} are s ensory and sensory-cortex outputs, respectively, and j is the jth input. Variations of V_j and W_j can be calculated as

$$\Delta V_i = \alpha[\max(0, Sc_j(R - \sum_i A_i))] \tag{38}$$

$$\Delta V_{th} = \alpha[\max(0, Sc_j(R - A_{th}))] \tag{39}$$

Moreover, likewise, the E' node sums the outputs from A except A_{th} and then subtracts from inhibitory outputs from the O nodes

$$E' = \sum_j A_j + A_{th} - \sum_j O_j \tag{40}$$

$$\Delta W_i = \beta[Sc_j - (E' - R)] \tag{41}$$

where (α,α_{th}) and β are the learning steps in the amygdala and orbitofrontal cortex, respectively. R is the value of the emotional cue function at each time. The learning rule of the amygdala is given in (39), which cannot decrease. It means that it does not forget the information in the amygdala, whereas idiomatically inhibiting (forgetting) is the duty of the orbitofrontal cortex (38). Eventually, the model output is obtained from (33).

Fig. 7 shows the BELBIC controller configuration [24].

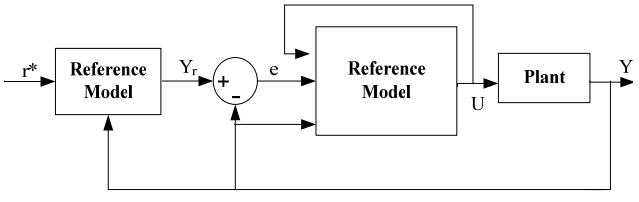

Fig. 7. Control system configuration using BELBIC.

The used functions in the emotional cue R and sensory input S blocks can be given by the following:

$$R = f(E, e.y, y_d) \tag{42}$$

$$S = G(y, y_d, e) \tag{43}$$

In this paper, functions f and g are given by

$$g = k_1 e + k_2 \frac{d}{dt} e + k_3 \int e.dt \tag{44}$$

$$f = K_1|e| + K_2|e.y| + K_3|y_p| \tag{45}$$

Where e, yp, and y are the system error, controller output, and system output, respectively. Also, $k1$ and $K1$, $k2$ and $K2$, as well as $k3$ and $K3$ are gains like in the PID controller, which must be tuned for designing as satisfactory controller given in the Appendix. Eventually, initial values for α and β in O and A and functions R and S should be selected for emotional signal generation [25].

In this paper, the proposed controller is modified by separating the learning process of the thalamic stimulus from the sensory cortex stimuli in the amygdala (38, 39). A simple lowpass filter is used for modeling the thalamus. The neurophysiological speed response in the sensory cortex is faster than that in the thalamus [23, 24].

4. Simulation

4.1 Single-machine system modeling

A single-machine system with an infinite bus (SMIB) has been shown in Fig. 8. In this paper, MATLAB/ SIMULINK software is used for simulating and modeling. Transient stability is studied during the first oscillation, and during this period, the critical clearing time (CCT) will be evaluated. In order to find the critical time of the fault removal, a step by step method has been used. In this way in which the fault duration is gradually increased to obtain the last time in which the system would be unstable.

Three-phase fault, which is the worst and most common fault in the practical power systems, has been considered for the whole simulations. The fault place is considered on the BUS-i. By this method, CCT has obtained 209 ms for SIMB system without any compensation. It is supposed that the fault has occurred on 7th second after the startup moment; because the system must be reached on the steady state of the permanent performance; otherwise, the shortest fault can also result in the system instability. Now, the method mentioned above, is repeated again to calculate CCT, but this time, IPFC has been placed in the network.

Supposing that IPFC is placed in the network with U_{T1} = 0.1 p.u. and U_{T2}= 0.1 p.u. Fig. 9 shows a system encountered a three-phase fault. The results have obtained supposing that the fault has lasted about 240 ms. Figs. 9(a)

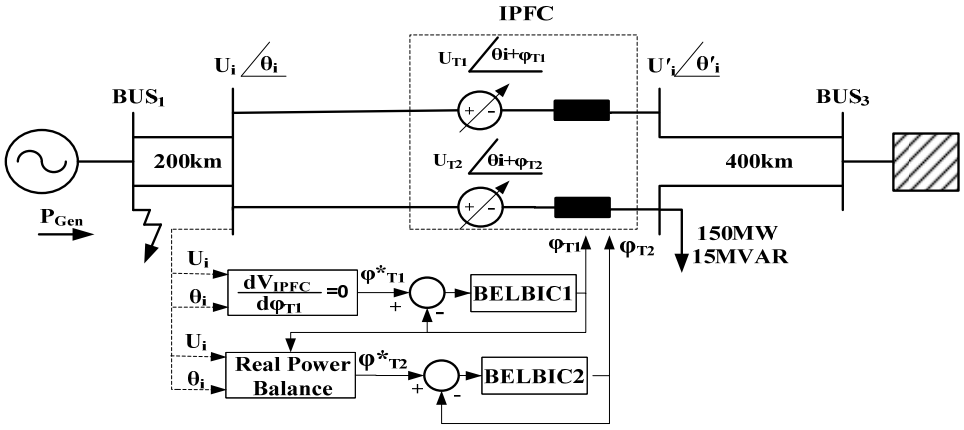

Fig. 8. SMIB system with IPFC and controllable blocks

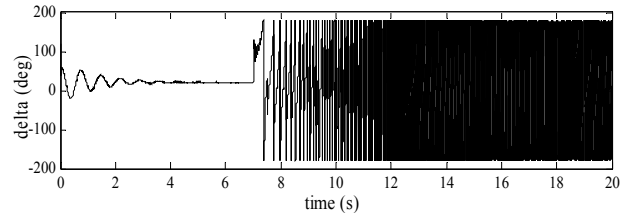

(a)

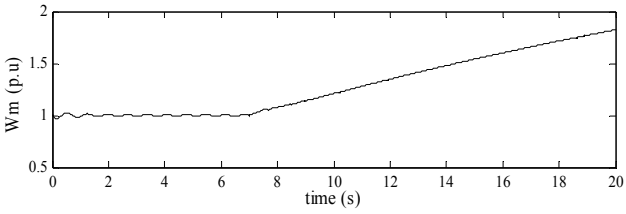

(b)

Fig. 9. Simulation results of the SMIB without any compensation: (a) machine angel; (b) machine speed

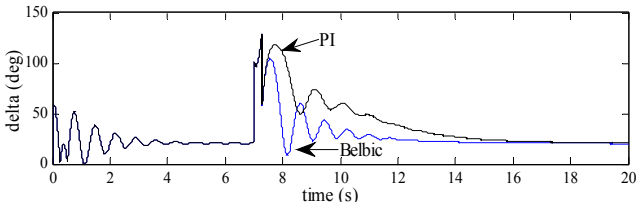

(a)

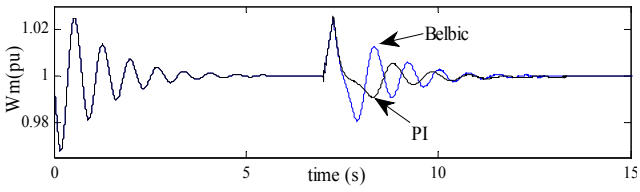

(b)

Fig. 10. Simulation results of the SMIB with IPFC in the error duration 242 ms: (a) machine angel; (b) machine speed

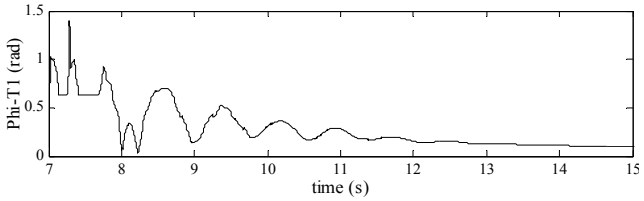

(a)

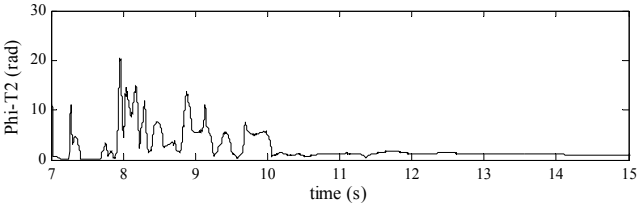

(b)

Fig. 11. BELBIC controllers output in the error duration 242 ms: (a) φ_{T1}; (b) φ_{T2}

and 9(b) show machine angel and machine speed without compensator respectively. The main idea of this method is to create the motor orbits under the different primary conditions in mechanical second-degree systems, and then to study the qualitative characteristics of these orbits. Because of being graphical, this method provides a relevant tool for observing the system behavior.

In Figs. 10(a) and 10(b) the speed and angle of the machine with compensator and PI and BELBIC controller have been respectivey shown in the error duration 240 ms. Figs. 10(a) in same error duration condition, shows the effect of BELBIC on the other transient stability standards that is the oscillations damping improvement and the overshot reduction.

Figs. 11(a) and 11(b) φ_{T1} and φ_{T2} obtained from BELBIC has been shown in order to maximize the energy function in the error duration 257 ms.

In Fig. 12 the system phase surface diagram has been shown in the error duration 257 ms. In Fig. 12(a) the system is stable using BELBIC controller but in Fig. 12(b)

Table 1. CCTs obtained in a SMIB with different value of U_T including an IPFC

U_{T1}(p.u)	U_{T2}(p.u)	CCT(ms)	
		BELBIC	PI
0	0	209	209
0.1	0.1	257	240
0.2	0.2	269	253
0.3	0.3	289	260
0.4	0.4	298	268

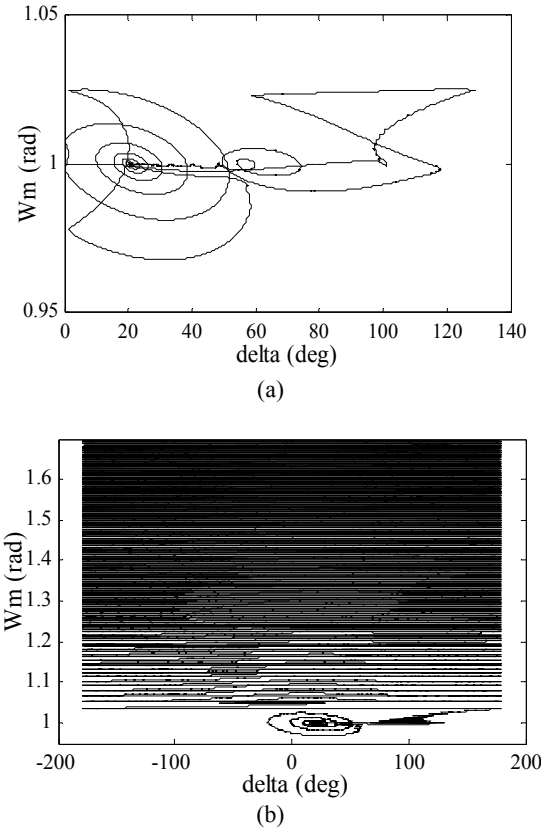

Fig. 12. System phase surface diagram with IPFC in the error duration 257 ms: (a) system is stable using BELBIC controller; (b) system is unstable using PI controller

PI controller could not preserve the system stability.

Table 1 shows CCT values obtained by the various values of U_{T1}, U_{T2} with PI controller and BELBIC.

4.2 Multi-machine system modeling

Standard 9-Bus single line diagram has been shown in Fig. 13. Like the single-machine state, by exerting three-phase fault to the system which its place has been shown in Fig. 13, by gradual increasing fault time duration, CCT is calculated. For a system without compensation, this time has obtained 117 ms. Here, the fault removal has accommodated by exiting the line from the network, thus, both oscillations and admittance matrix will be different after the fault.

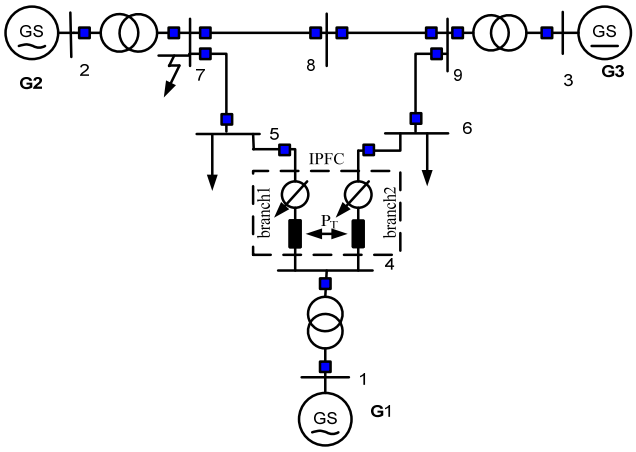

Fig. 13. standard 9-buses system single line diagram

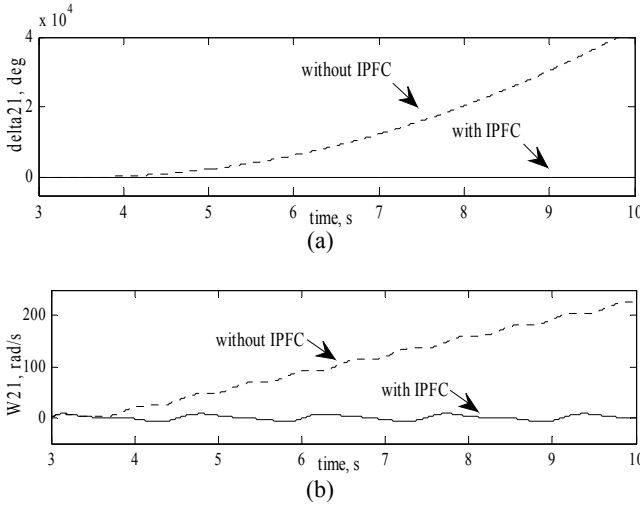

Fig. 14. Simulation results of the 9-buses system with and without compensation in the error duration 129 ms: (a) relative angular position δ_{21}; (b) relative angular speed ω_{21}

When the system, applies IPFC in order to improve the transient stability, it performs as a compensator, its impression must be modeled in some way. Thus, two changes will occur on the main system: first, fault occurrence, and second, entering IPFC to the network. The fault occurrence is modeled by changing the admittance matrix and calculating it on three time periods, and naturally, the power changes. In order to study IPFC in the network, its impression has been directly considered on the network powers. In this manner, the real power injected by IPFC has an impact on the generators' real powers (directly on the generator 1, and indirectly on the other generators), and therefore, it results in improving the operation. In order to compare a system encountered a fault with duration of 129 ms, the system variables have been shown on two conditions in Fig. 14. In Figs. 14(a) and 14(b) relative angular position and speed with and without compensator.

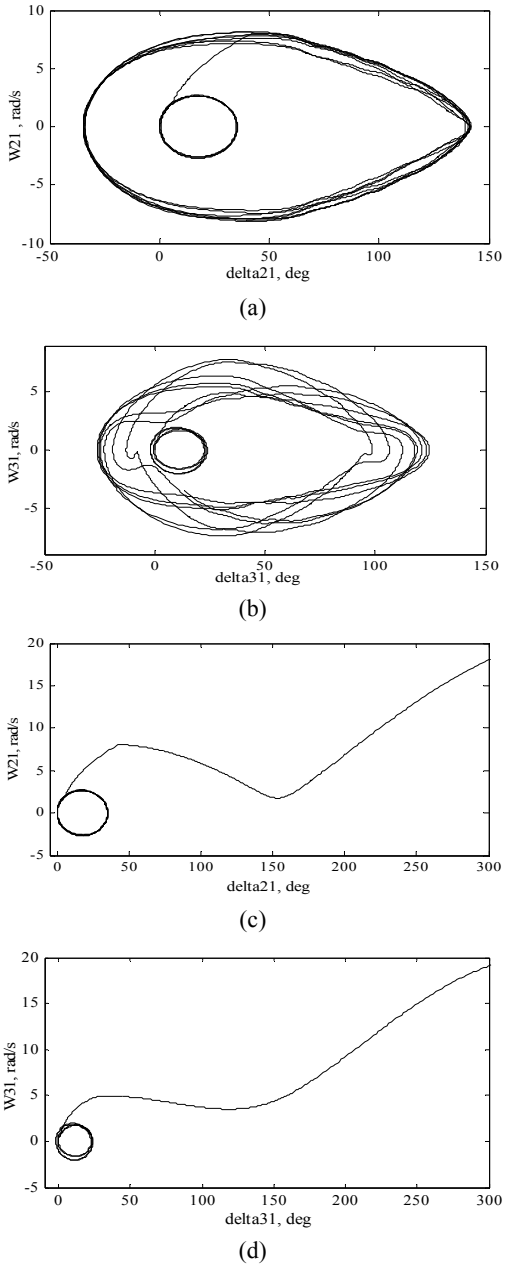

Fig. 15. System phase surface diagram with IPFC in the error duration 135 ms: (a), (b) system is stable using BELBIC controller; (c), (d) system is unstable using PI controller

Here, this state is similar to the single-machine state in which the system has reached on the steady state, and then, the fault has occurred. Selecting the place has accomplished just by examining two other states, and consequently, the selected place, marked on Fig. 13, shows the more CCT increasing toward two other places. IPFC control method, for a multi-machine system, has been exactly considered like a single-machine system to verify its efficiency also for the multi-machine system. Because the methods are alike, it is prevented from the repetition. In Fig. 15 the system phase surface diagram has been shown

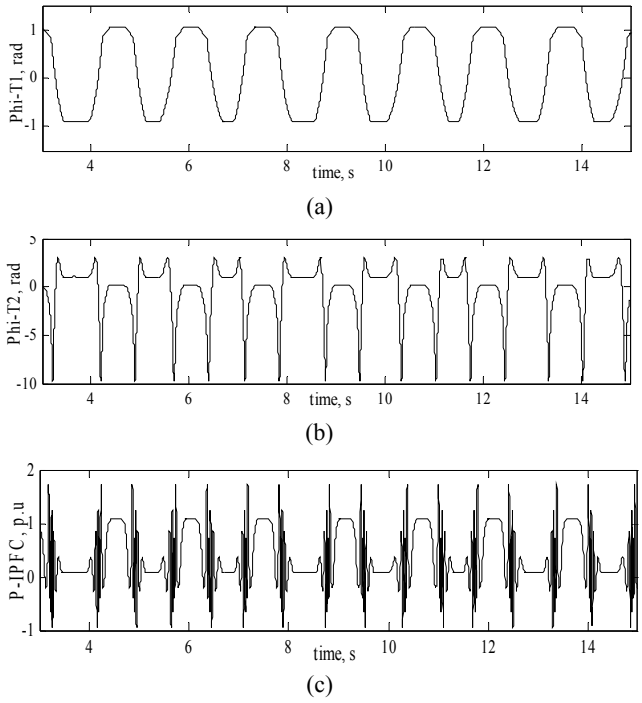

Fig. 16. BELBIC controllers output in the error duration 135 ms: (a) φ_{T1}; (b) φ_{T2}; (c) active-power injection by IPFC

Table 2. CCTs obtained in a standard 9-buses system with different value of U_T including an IPFC

U_{T1}(p.u)	U_{T2}(p.u)	CCT(ms)	
		BELBIC	PI
0	0	117	117
0.1	0.1	139	129
0.2	0.2	143	133
0.3	0.3	150	137
0.4	0.4	156	141

in the error duration 135 ms. in Figs. 15(a) and 15(b) the system is stable using BELBIC controller but in Figs. 15(c) and 15(d) PI controller could not preserve the system stability. Emotional Intelligent controllers output, which is the same series branches voltage angle and IPFC power, has been shown on Figs. 16(a), (b) and (c) respectively. Table 2 shows CCT values obtained by the various valaes of U_{T1}, U_{T2} with PI and BELBIC controllers.

5. Conclusion

In this paper, the transient stability improvement has been studied using IPFC with PI and BELBIC controllers. The application of IPFC with Belbic controller to improve the transient stability is more effective than PI controller. The emotional intelligent controller with a model free and simple structure has a better affect on the oscillation damping, overshot reduction and CCT improvement.

Computer simulation tests show the effectiveness and superiority of BELBIC, in the multi-machine and single-machine system.

Appendixe

Table 3, 4 shows Simulation parameters of SMIB and multi- machine system.

Gain parameters for BELBICare: α=1.5e-2, α_{Th}=2e-2, β=4e-2, *K1*=0.32, *k1*=0, *K2*=0. 1, *k2*=0.02, *K3*=0.1, *k3*=0.8.

Table 3. Simulation parameters of SMIB

H (MJ/MVA)	3.12	K_E	-0.243
X_d (p.u)	0141.	T_E (sec)	0.95
X_q (p.u)	6.0	K_F	0.05
X'_d (p.u)	3140.	T_F (sec)	0.35
T'_{do} (sec)	556.	K_D	2
K_A	400	X_T (p.u)	0.07
T_A (sec)	05.0	X_L (p.u)	0.65

Table 4. Simulation parameters of multi- machine system

Generator no.	1	2	3
Type	Hydro	Steam	Steam
Rate(MVA)	247.5	192	128
(Kv)	16.5	18	13.8
Power factor	1	0.85	0.85
H	23.64	6.4	3.01
X_d (p.u)	0.146	0.9	1.3125
X'_d (p.u)	0.0608	0.12	0.1813
X_q (p.u)	0.097	0.8645	1.2578
X'_q (p.u)	0.097	0.197	0.25
T_{do} (sec)	8.96	6	5.9
T'_{qo} (sec)	0	0.535	0.6
X_l (p.u)	0.0336	0.0521	0.074

Refrence

[1] Hingorani, N.G and Gyugyi, L., "Understanding FACTs: Concepts and technology of flexible ac transmission systems", *IEEE Press, NY*, 1999.

[2] R. Mihalic, P. Zunko, D. Povh, "Improvement of transient stability using unified power flow controller", *IEEE Trans. Power Delivery,* Vol. 11, No. 1, pp. 485-492, Jan. 1996.

[3] A. Nabavi-Niaki, M. R. Iravani, "Steady State and Dynamic of Unified Power Flow Controller (UPFC) for Power System Studies", IEEE Trans. Power Systems, Vol. 11, No. 4, pp. 1937-1943, Nov.1996.

[4] M. H. Haque, "Application of UPFC to Enhance Transient Stability Limit", *IEEE Power Eng. Society General Meeting*, pp. 1-6, June 2007

[5] N. Narasimhamurthi, M. R. Musavi, "A General Energy Function for Transient Stability Analysis", IEEE Trans. CAS, Vol. CAS-31, No.7, pp. 637-675, July 1984.

[6] T. Athay, R. Podmore, S. Virmani, "A Practical Method for the Direct Analysis of Transient Stability", *IEEE Trans. PAS,* pp. 573-584, March/April 1979.

[7] N. Kakimoto, M. Hayashi, "Transient Stability Analysis of Multimachine Power System by Lyapunov's Direct Method", Proc. *20th IEEE Conf. on Decision and Control*, 1981.

[8] Th. V. Cutsem, M. Ribbens-Pavella, "Structure preserving direct methods for transient stability analysis of power systems", Proc. 24th Conf. on Decision and Control, pp 70-77, Dec. 1985.

[9] V. Azbe, U. Gabrijel, D. Povh, R. Mihalic, "The Energy Function of a General Multimachine System With a Unified Power Flow Controller", *IEEE Trans. Power Systems*, Vol. 20, No. 3, August 2005.

[10] M. Januszewski, J. Machowski, J. W. Bialek, "Application of the Direct Lyapunov Method to Improve Damping of Power Swings by Control of UPFC", *IEE Proc.-Gener. Transm. Distrib*, Vol. 151, No. 2, pp. 252-260, March 2004.

[11] L. Gyugyi, K.K. Sen, C.D. Schauder, "The interline power flow controller concept: a new approach to power flow management in transmission systems," *IEEE Trans. Power Deliv*. 14 (1999) 1115-1123.

[12] R. Mihalic, "Power flow control with controllable reactive series elements," *IEE Proceedings-Generation, Transmission and Distribution* 145(1998) 493-498.

[13] M. Noroozian, L. Angquist, G. Ingestrom, "Series compensation," Y. H. Song, A. T. Johns (Eds.), Flexible ac Transmission Systems (FACTs), *IEE, London*, U.K., 1999, pp. 199-242.

[14] S. Teerathana, A. Yokoyama, "An optimal power flow control method of power system using interline power flow controller (IPFC)," Proceedings of IEEE Region 10 Conference, TENCON 2004, 2004, pp. 343-346.

[15] X. Wei, J. H. Chow, B. Fardanesh, A. A. Edris, "A dispatch strategy for an interline power flow controller operating at rated capacity," Proceedings of IEEE/ PES Power Systems Conference and Exposition 2004, 2004, pp. 1459-1466.

[16] B. Fardanesh, "Optimal utilization, sizing, and steady-state performance comparison of multiconverter VSC-based FACTs controllers," IEEE Trans. Power Deliv.19 (2004) 1321-1327.

[17] V. Azbe, R. Mihalic, "Energy function for an interline power-flow controller," Electric Power Systems Research 79 (2009) 945-952.

[18] S. Limyingcharoen, U. D. Annakkage, N. C. Pahalawaththa, "Fuzzy Logic Based Unified Power Flow Controllers for Transient Stability Improvement", IEE Proc.-Gener. Transm. Distrib., Vol. 145, No. 3, May 1998.

[19] S. Mishra, "Neural-network-based Adaptive UPFC for Improving Transient Stability Performance of Power System", *IEEE Trans. Neural Networks*, Vol.

17, No. 2, pp. 461-470, March 2006.

[20] Chia-Chi Chu, Hung-Chi Tsai, "Application of Lyapunov-Based Adaptive Neural Network Controllers for Transient Stability Enhancement," *Power and Energy Society General Meeting,* pp. 1-6, July 2008.

[21] V. K. Chandrakar, A. G. Kothari, "Comparison of RBFN based STATCOM, SSSC and UPFC Controllers for Transient Stability Improvementm," *Power Systems Conference and Exposition*, pp. 784-791, Nov. 2006.

[22] M. R. Jamaly, A. Armani, M. Dehyadegari, C. Lucas, and Z. Navabi, "Emotion on FPGA: Model driven approach," *Expert Syst. Appl.*, vol. 36,no. 4, pp. 7369-7378, May 2009.

[23] J. Moren, "Emotion and learning: A computational model of the Amygdala," Ph.D. dissertation, Lund Univ., Lund, Sweden, 2002.

[24] J. Moren and C. Balkenius, "A computational model of emotional learning in the amygdala," in *Proc. 6th Int. Conf. Simul. Adapt. Behav.*, Cambridge, MA, 2000, pp. 411-436.

[25] C. Lucas, D. Shahmirzadi, and N. Sheikholeslami, "Introducing BELBIC : Brain emotional learning based intelligent control," *Int. J. Intell. Automat. Soft Comput.*, Vol. 10, No. 1, pp. 11-22, 2004.

[26] N. Sheikholeslami, D. Shahmirzadi, E. Semsar, C. Lucas, and M. J. Yazdanpanah, "Applying brain emotional learning algorithm for multivariable control of HVAC systems," *J. Intell. Fuzzy Syst.*, Vol. 17, No. 1, PP. 35-46, 2006.

[27] H. Rouhani, M. Jalili, B. Arabi, W. Eppler, and C. Lucas, "Brain emotional learning based intelligent controller applied to neurofuzzy model of micro-heat exchanger," *Expert Syst. Appl.*, Vol. 32, No. 3, pp. 911-918, 2007.

[28] R. M. Milasi, C. Lucas, and B. N. Araabi, "Intelligent modeling and control of washing machine using locally linear neuro-fuzzy (LLNF) modeling and modified brain emotional learning based intelligent controller(BELBIC)," *Asian J. Control*, Vol. 8, No. 4, pp. 393-400, Dec. 2006.

[29] R. M. Milasi, M. R. Jamali, and C. Lucas, "Intelligent washing machine: A bioinspired and multi-objective approach," *Int. J. Control Automat. Syst.*, Vol. 5, No. 4, pp. 436-443, Aug. 2007.

[30] M. R. Jamali, M. Valadbeigi, M. Dehyadegari, Z. Navabi, and C. Lucas, "Toward embedded emotionally intelligent system," in *Proc. IEEE EWDTS*, Sep. 2007, pp. 51-56.

[31] M. R. Jamali, A. Arami, B. Hosseini, B.Moshiri, and C. Lucas, "Real time emotional control for anti-swing and positioning control of SIMO overhead traveling crane," *Int. J. Innovative Comput. Inf. Control*, Vol. 4, No. 9, pp. 2333-2344, Sep. 2008.

[32] M. R. Jamali, M. Dehyadegari, A. Arami, C. Lucas, and Z. Navabi, "Realtime embedded emotional controller," *J. Neural Comput. Appl.*, Vol. 19, No. 1, pp. 13-19, 2010.

[33] M. A. Rahman, R. M. Milasi, C. Lucas, B. N. Arrabi, and T. S. Radwan,"Implementation of emotional controller for interior permanent magnet synchronous motor drive," *IEEE Trans. Ind. Appl.*, Vol. 44, No. 5, pp. 1466-1476, Sep./Oct. 2008.

[34] G. R. Arab Markadeh, E. Daryabeigi, C. Lucas, and M. A. Rahman, "Speed and Flux Control of Induction Motors Using Emotional Intelligent Controller," *IEEE Trans. Ind. Appl.*, Vol. 47, No. 3, pp. 1126-1135, MAY/JUNE 2011.

[35] E. Daryabeigi, G. Arab Markadeh, C. Lucas, "Emotional controller in Electric Drives – A Review", *IEEE Conf, IECON* 2010, pp. 2901 - 2907 Nov., 2010.

[36] Mohammdi-Milasi, R.; Lucas, C.; Najar-Arrabi, B.; a novel controller for a power system based belbic (Brain Emotional Learning Based Intelligent, Controller) *Proceeding Automation Congress,* 2004*,* pp. 409-420.

[37] E. T. Rolls, *The Brain and Emotion*. London, U.K.: Oxford Univ. Press, 1999.

Ehsan jafari was born in Shahrekord, Iran. He received the M.Sc degree in Power systems from the Islamic Azad University of najafabad, Iran, in 2011. Now, he is student of PHD level at the Department of Electrical Engineering, Islamic Azad University of science and Research Branch, Tehran, Iran. His interests include FACTS devices, DTC and nonlinear control.

Ali Marjanian was born in Shahrekord, Iran. He received the degree in Electrical Engineering from the University of Shahrekord, Iran, in 2008, and received the M.Sc degree in Power systems from the Islamic Azad University of Dezfol, Iran, in 2011. Now, he is student of PHD level at the Department of Electrical Engineering, Islamic Azad University of science and Research Branch, Tehran, Iran. His interests include FACTS devices, transient stability, reactive power compensation, and power distribution systems.

Soodabeh Soleymani (M'1977, Feb'18) received her B.S and M.S degrees in electrical engineering from the Sharif University of Technology. Since 2004, She is pursuing her PhD program at the same university. Her area of research includes power market simulation, and market power monitoring in deregulated power systems.

Ghazanfar Shahgholian was born in Isfahan, Iran, on December 7, 1968. He graduated in Electrical Engineering from Isfahan University of Technology, Isfahan, Iran, in 1992. He received the M.Sc and Ph.D. degrees in Electrical Engineering from University of Tabriz, Tabriz, Iran in 1994 and from Science and Research Branch, Islamic Azad University, Tehran, Iran, in 2006, respectively. He is now an associate professor at Department of Electrical engineering, Faculty of engineering, Islamic Azad University Najafabad Branch. His teaching and research interests include application of control theory to power system dynamics, power electronics and power system simulation.